LabVIEW Event Detection using Pan –Tompkins Algorithm

MIHAELA LASCU, DAN LASCU
Department of Measurements and Optical Electronics
Faculty of Electronics and Telecommunications
Bd. Vasile Pârvan no.2
ROMANIA

http://www.etc.upt.ro

Abstract: - QRS and ventricular beat detection is a basic procedure for electrocardiogram (ECG) processing and analysis. Large variety of methods have been proposed and used, featuring high percentages of correct detection. Nevertheless, the problem remains open especially with respect to higher detection accuracy in noisy ECGs. LabVIEW (Laboratory Virtual Instrument Engineering Workbench) is a graphical programming language that uses icons instead of lines of text to create programs. We developed in LabVIEW the filtering for removal of artifacts in biomedical signals and the Pan-Tompkins algorithm. We have investigated problems posed by artifact, noise and interference of various forms in the acquisition and analysis of several biomedical signals. We have also established links between the characteristics of certain epochs in a number of biomedical signals and the corresponding physiological or pathological events in the biomedical systems of concern. Event detection is an important step that is required before we may attempt to analyze the corresponding waves in more detail.

Key-Words: - biomedical signal, database, electrocardiogram ECG, artifact, noise, graphical programming language LabVIEW, filtering, notch filter, event detection, Pan-Tompkins algorithm.

1. Introduction

Biomedical signals are fundamental observations for analyzing the body function and for diagnosing a wide spectrum of diseases.

The problems caused by artifacts in biomedical signals are vast in scope and variety; their potential for degrading the performance of the most sophisticated signal processing algorithms is high.

An ECG signal [1] can be disturbed by a high-frequency noise. The noise could be due to the instrumentation amplifiers, the recording system, pickup of ambient electromagnetic signals by the cables. The signal illustrated has also been corrupted by power-line interference at 60Hz and its harmonics, which may also be considered as a part of high-frequency noise relative to the low-frequency nature of the ECG signal.

Low-frequency artifacts and base-line drift may be caused in chest-lead ECG signals by coughing or breathing with large movement of the chest. Poor contact and polarization of the electrodes may also cause low-frequency artifacts. Base line drift may sometimes be caused by variations in temperature and bias in the instrumentation and amplifiers as well.

The most commonly encountered periodic artifact in biomedical signals is the power-line interference at 50Hz or 60Hz. If the power-line waveform is not a pure sinusoid due to distortions or clipping, harmonics of the fundamental frequency could also appear. Harmonics will also appear if the interference is a periodic waveform that is not a sinusoid. Power-line interference may be difficult to detect visually in signals being non-specific waveforms; however, the interference is easily visible if present on well-defined signal waveforms such as the ECG or carotid pulse signals. In either case, the power spectrum of the signal should provide a clear indication of the presence of power-line interference as an impulse or spike at 50Hz or 60 Hz; harmonics will appear as additional spikes at integral multiples of the fundamental frequency.

If we have an ECG signal recorded from the abdomen of a pregnant woman and simultaneously a recorded ECG from the woman's chest; and we compare these, we see that the abdominal ECG demonstrates multiple peaks corresponding to the maternal ECG as well as several others at weaker levels and higher repetition rate [1].

The non-maternal QRS complexes represent the ECG of the fetus. Observe that the QRS complex shapes of the maternal ECG from the chest and abdominal leads have different shapes due to the projection of the cardiac electrical vector onto different axes.

The QRS complexes and ventricular beats in an electrocardiogram represent the depolarization phenomenon of the ventricles and yield useful information about their behavior. Beat detection is a procedure preceeding any kind of ECG processing and analysis. For morphological analysis this is the reference for detection of other ECG waves and parameter measurements. Rhythm analysis requires classification of QRS and other ventricular beat complexes as normal and abnormal. Real-time ventricular beat detection is essential for monitoring of patients in critical heart condition.

2. Filtering for Removal of Artifacts

Information provided by bioelectric signals are generally time-varying, nonstationary, sometimes transient, and usually corrupted by noise. Fourier transform has been the unique tool to face such situations, even if the discrepancy between theoretical considerations and signal properties has been emphasized for a long time. These issues can be now nicely addressed by time-scale and time-frequency analysis.

One of the major areas where new insights can be expected is the cardiovascular domain. For diagnosis purpose, the noninvasive electrocardiogram ECG is of great value in clinical practice. The ECG is composed of a set of waveforms resulting from atrial and ventricular depolarization and repolarization. The first step towards ECG analysis is the inspection of P, QRS and T waves Fig.1; each one of these elementary components is a series of onset, offset, peak, valley and inflection points. Ideally, the waves exhibit local symmetry properties with respect to a particular point, peak and inflection points locations of the considered wave. Based on these properties, one can extract significant points to study the wave shapes and heart rate variability.

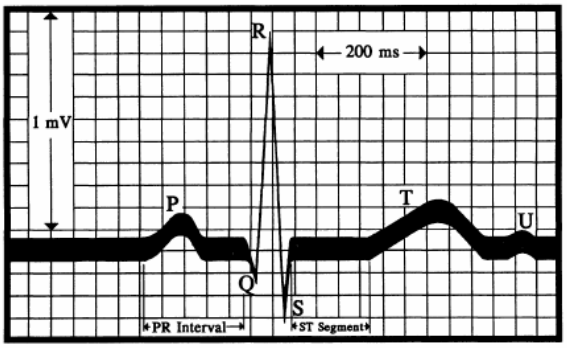

Fig.1. Example of a normal ECG beat.

In our paper we have gained an understanding of a few sources of artifacts in biomedical signals and their nature and we are prepared to look at specific problems and develop effective filtering techniques to solve them. The proposed solution provides the details of an appropriate filtering technique. Certain types of noise may be filtered directly in the time domain using signal processing techniques or digital filters. An advantage of time-domain filtering is that spectral characterization of the signal and noise may not be required. Linear filters fail to perform when the signal and noise spectra overlap. Synchronized signal averaging can separate a repetitive signal from noise without distorting the signal [1]. A synchronized averaging is a type of ensemble averaging. An algorithmic description of synchronized averaging is as follows: a) obtain a number of realizations of the signal or event of interest; b) determine a reference point for each realization of the signal; c) extract parts of the signal corresponding to the events and add them to the buffer, it is possible that the different parts are of different durations; d) divide the result in the buffer by the number of events added.

Let $y_k(n)$ represent one realization of a signal, with $k = 1,2,\ldots, L$ representing the ensemble index, and $n = 1,2,\ldots, N$ representing the time-sample index. The observed signal is

$$y_k(n)=x_k(n)+\eta_k(n), \qquad (1)$$

where $x_k(n)$ represents the original uncorrupted signal and $\eta_k(n)$ represents the noise in the kth copy of the observed signal. If for each instant of time n we add L copies of the signal, we get

$$\sum_{k=1}^{L} y_k(n)=\sum_{k=1}^{L} x_k(n)+\sum_{k=1}^{L} \eta_k(n);\ n=1,2,\ldots,N. \qquad (2)$$

If the repetitions of the signal are identical and aligned, $\sum_{k=1}^{L} x_k(n)=Lx(n)$. If the noise is random and has zero mean and variance σ_η^2, $\sum_{k=1}^{L} \eta_k(n)$ will tend to zero as L increases, with a variance of $M\sigma_\eta^2$. The RMS value of the noise in the averaged signal is $\sqrt{M}\sigma_\eta$. Thus the SNR of the signal will increase by a factor of $\frac{L}{\sqrt{L}}$ or $\sqrt{L}$. The larger the number of epochs or realizations that are averaged, the better will be the SNR of the result.

Fig.2 illustrates two ECG cycles extracted using the trigger points obtained by thresholding the cross-correlation function [1], as well as the result of averaging the first 11 cycles in the signal.

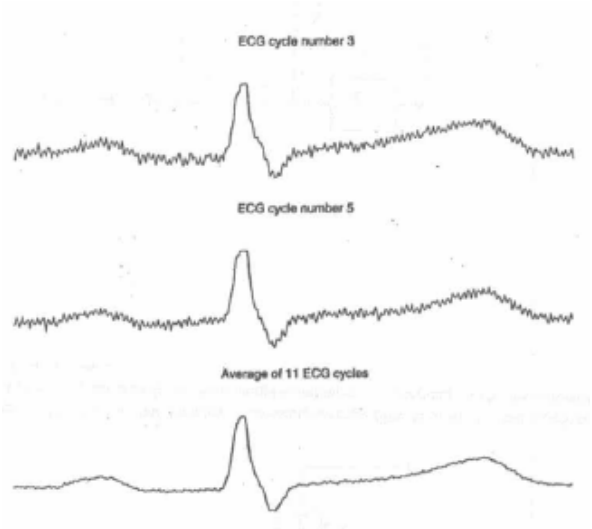

Fig.2. The upper two traces - two cycles of the ECG extracted from an ECG signal with noise. The bottom trace – the result of synchronized averaging of 11 cycles from the same ECG signal.

Structured noise such as power-line interference may be suppressed by synchronized averaging if the phase of the interference in each realization is different.

When an ensemble of several realizations of an event is not available, synchronized averaging will not be possible. In this case we consider temporal averaging for noise removal, with the assumption that the processes involved are ergodic, that is, temporal statistics may be used instead of ensemble statistics.

The biomedical signals, that have been processed , are from Online Biomedical Signals Databases: ftp://ftp.ieee.org/uploads/press/rangayyan, www.ecgdatabase.com, www.ecglibrary.com.

2.1 High frequency noise in the ECG.

The Butterworth filter is perhaps the most commonly used frequency domain filter due to its simplicity and the property of a maximally flat magnitude response in the pass-band [2].

The basic Butterworth lowpass filter function is:

$$\left|H_a(j\Omega)\right|^2 = \frac{1}{1+\left(\frac{j\Omega}{j\Omega_c}\right)^{2N}}\left|H_a\right| \qquad (3)$$

where H_a is the frequency response of the analog filter and Ω_c is the cutoff frequency in radians/s and N is the order of the filter. As the order N increases, the filter response becomes more flat in the pass-band, and the transition to the stop-band becomes faster or sharper.

Changing to the Laplace variable s, we get:

$$H_a(s) * H_a(-s) = \frac{1}{1+(\frac{s}{j\Omega_c})^{2N}}; \qquad (4)$$

Using the bilinear transformation, that means, by substituting $s = \frac{2}{T}\frac{1-z^{-1}}{1+z^{-1}}$, we obtain the following simplified transfer function:

$$H(z) = \frac{G'\left(1+z^{-1}\right)^N}{\sum_{k=0}^{N} a_k z^{-k}} \qquad (5)$$

where a_k , k=0,1,2,…,N, are the filter coefficients and G' is the gain factor at z=1. The filter is now in the familiar form of an IIR filter. A form of realization of a generic IIR filter is illustrated as signal-flow diagram in Fig.3.

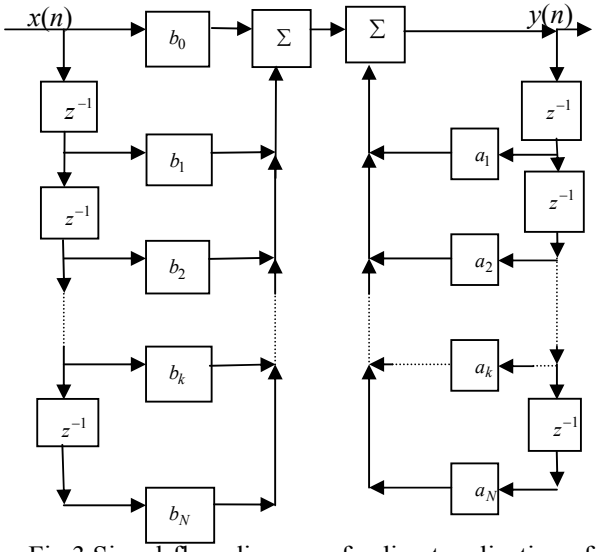

Fig.3.Signal-flow diagram of a direct realization of a generic infinite impulse response filter.

Following LabVIEW program based on the IIR filter for eliminating the high frequency noises was realized and the graphs concerning the input signal and the output signal processed with the IIR filter are presented in Fig.4.

2.2 Low frequency noise in the ECG

Low-frequency artifacts and base-line drift may be caused in chest-lead ECG signals by coughing or breathing with large movement of the chest. Poor contact and polarization of the electrodes may also cause low-frequency artifacts. Base line drift may sometimes be caused by variations in temperature and bias in the instrumentation and amplifiers as well.

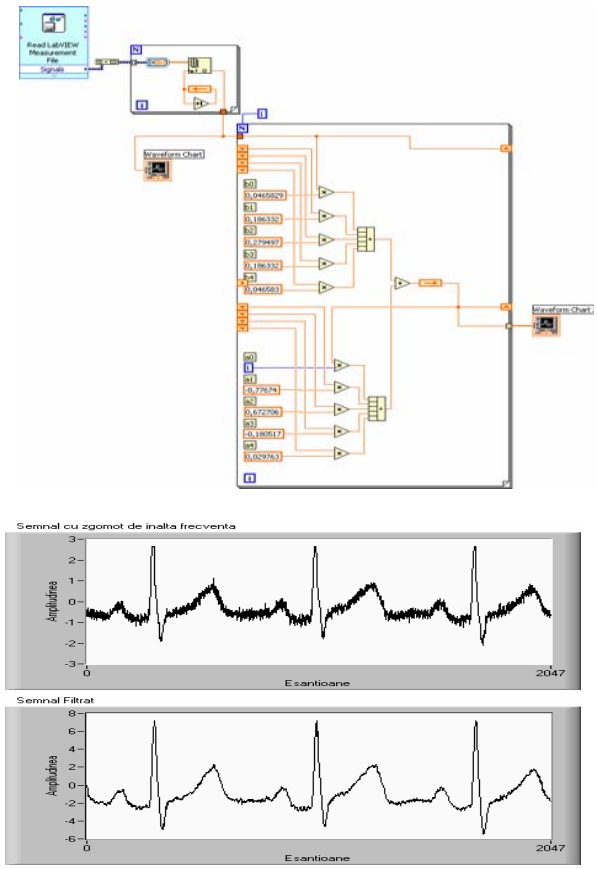

Fig.4.LabVIEW program based on IIR filter, high frequency noise signal upper graph and filtered signal lower graph (x-samples, y-amplitude).

The drawback of the first-order difference and the three-point central-difference operators [1] lies in the fact that their magnitude responses remain low for a significant range of frequencies well beyond the band related to base-line wander. We would like to maintain the levels of the components present in the signal beyond about 0.5-1Hz, that is, we would like the gain of the filter to be close to unity after about 0.5Hz. The gain of a filter at specific frequencies may be boosted by placing poles at related locations around the unit circle in the z-plane. For the sake of stability of the filter, the poles should be placed within the unit circle. Since we are interested in maintaining a high gain at very low frequencies, we could place a pole on the real axis (zero frequency), at say z=0.995 [2]. The transfer function of the modified first-order difference filter is then

$$H(z) = \frac{1}{T}\left[\frac{1 - z^{-1}}{1 - 0.995 z^{-1}}\right] \qquad (6)$$

or

$$H(z) = \frac{1}{T}\left[\frac{z - 1}{z - 0{,}995}\right] \qquad (7)$$

The time-domain input-output relationship is given as:

$$y(n) = \frac{1}{T}\left[x(n) - x(n-1)\right] + 0{,}995\, y(n-1) \qquad (8)$$

LabVIEW program and the obtained waveforms are the following, represented in Fig.5:

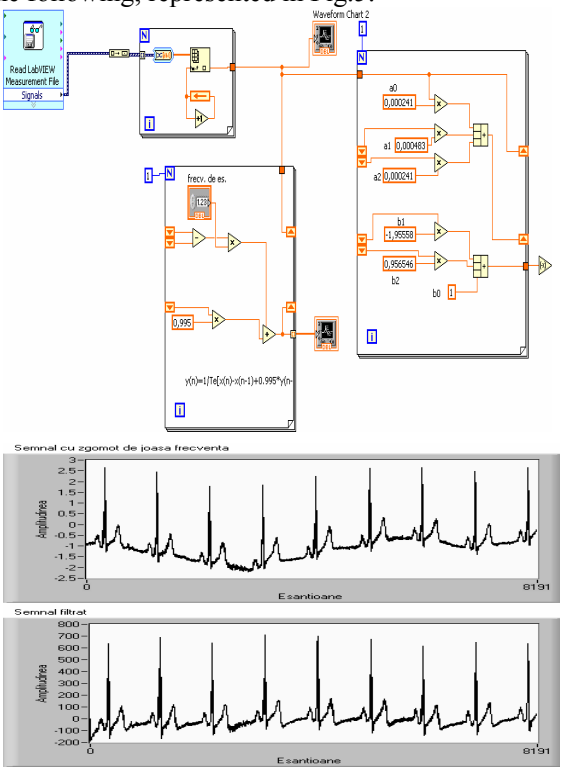

Fig.5.LabVIEW program based on the derivative operator, low frequency noise signal upper graph and filtered signal lower graph (x-samples, y-amplitude).

2.3 Power-line interference in ECG signals

The simplest method to remove periodic artifacts is to compute the Fourier transform of the signal, delete the undesired components from the spectrum, and then compute the inverse Fourier transform. The undesired components could be set to zero, or better, to the average level of the signal components over a few frequency samples around the component that is to be removed.

Periodic interference may also be removed by notch filters [1] with zeros on the unit circle in the z-domain at the specific frequencies to be rejected. Applying the LabVIEW program we obtain Fig.5:

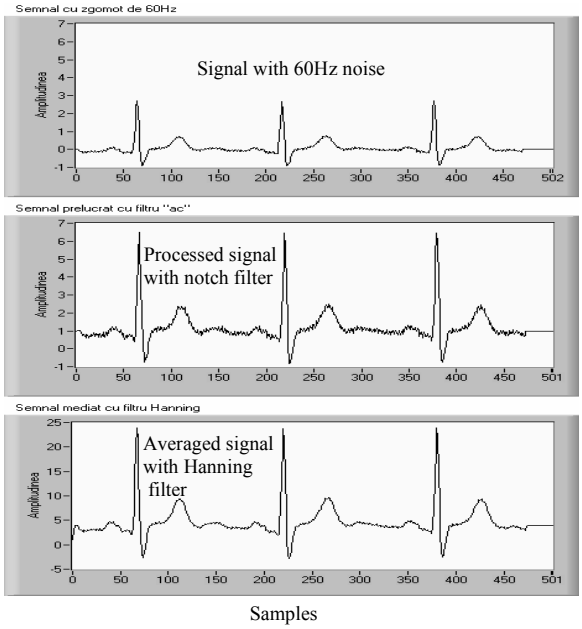

Fig. 5. Random noise elimination using notch filter and Hanning filter.

3 The Pan-Tompkins algorithm for QRS detection

Pan and Tompkins [3], [4] proposed a real-time QRS detection algorithm based on analysis of the slope, amplitude and width of QRS complexes. The algorithm includes a series of filters and methods that perform lowpass, highpass, derivative, squaring, integration, adaptive thresholding and search procedures Fig.6. In this paper we implemented the Pan-Tompkins algorithm for QRS detection [1] in LabVIEW.

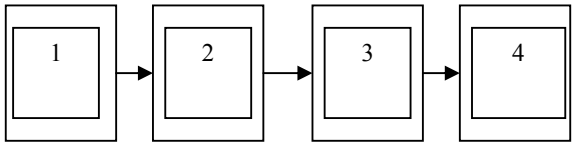

1: Band pass filter 2: Differentiator

3: Squaring operation 4: Moving-window integrator

Fig.6. Block diagram of the Pan-Tompkins Algorithm for QRS detection.

Lowpass filter: The recursive lowpass filter used in the Pan-Tompkins algorithm has integer coefficients for reducing computational complexity, with the transfer function defined as:

$$H(z)=\frac{1}{32}\cdot\frac{\left(1-z^{-6}\right)^2}{\left(1-z^{-1}\right)^2} \tag{9}$$

The output $y(n)$ is related to the input $x(n)$ as:

$$y(n)=2y(n-1)-y(n-2)+ \\ +\frac{1}{32}\left[x(n)-2x(n-6)+x(n-12)\right]. \tag{10}$$

With the sampling rate being 200 *Hz*, the filter has a rather low cutoff frequency of f_c=11Hz, and introduces a delay of 5 samples or 24*ms*. The filter provides an attenuation greater than 35*dB* at 60*Hz*, and effectively supresses power-line interference, if present.

Highpass filter: The highpass filter used in the algorithm is implemented as an allpass filter minus a lowpass filter. The lowpass component has the transfer function

$$H_{lp}(z)=\frac{1-z^{-32}}{1-z^{-1}} \tag{11}$$

the input-output relationship is:

$$y(n)=y(n-1)+x(n)-x(n-32). \tag{12}$$

The transfer function $H_{hp}(z)$ of the highpass filter is specified as:

$$H_{hp}(z)=z^{-16}-\frac{1}{32}H_{lp}(z). \tag{13}$$

The output $p(n)$ of the highpass filter is given by the difference equation

$$p(n)=x(n-16)-\frac{1}{32}\left[y(n-1)+x(n)-x(n-32)\right], \tag{14}$$

where $x(n)$ and $y(n)$ being related as in (12). The highpass filter has a cutoff frequency of 5*Hz* and introduces a delay of 80*ms*.

Derivative operator: The derivative operation used by Pan and Tompkins is specified as:

$$y(n)=\frac{1}{8}\left[2x(n)+x(n-1)-x(n-3)-2x(n-4)\right], \tag{15}$$

and approximates the ideal $\frac{d}{dt}$ operator up to 30 *Hz*. The derivative procedure suppresses the low-frequency components of the P and T waves, and provides a large gain to the high-frequency components arising from the high slopes of the QRS complex.

Squaring: The squaring operation makes the result positive and emphasizes large differences resulting from QRS complexes; the small differences arising from P and T waves are suppressed. The high-frequency components in the signal related to the QRS complex are further enhanced.

Integration: As observed in the previous subsection, the output of a derivative-based operation will exhibit multiple peaks within the duration of a single QRS complex. The Pan-Tompkins algorithm performs smoothing of the

output of the preceding operations through a moving-window integration filter as:

$$y(n)=\frac{1}{N}[x(n-(N-1))+x(n-(N-2))+...+x(n)].(16)$$

The choice of the window width N is to be made with the following considerations: too large a value will result in the outputs due to the QRS and T waves being merged, whereas too small a value could yield several peaks for a single QRS. A window width of N=30 was found to be suitable for $f_s = 200Hz$.

Adaptive thresholding: The thresholding procedure in the Pan-Tompkins algorithm adapts to changes in the ECG signal by computing running estimates of signal and noise peaks. A peak is said to be detected whenever the final output changes direction within a specified interval. *SPKI* represents the peak level that the algorithm has learned to be that corresponding to QRS peaks and *NPKI* represents the peak level related to non-QRS events.*THRESHOLDI1* and *THRESHOLDI2* are two thresholds used to categorize peaks detected as signal or noise. Every new peak detected is categorized as a signal peak or a noise peak. If a peak exceeds *THRESHOLDI1* during the first step of analysis, it is classified as a QRS peak. Using the searchback technique the peak should be above *THRESHOLDI2* to be called a QRS. The peak levels and thresholds are updated after each peak is detected and classified as:

SPKI = 0.125*PEAKI* + 0.875*SPKI* if *PEAKI* is a signal peak;

NPKI = 0.125*PEAKI* + 0.875*NPKI* if *PEAKI* is a noise peak;

THRESHOLDI1=NPKI + 0.25(*SPKI* - *NPKI*);

THRESHOLDI2=0.5*THRESHOLD I1*

The updating formula for *SPKI* is changed to

SPKI = 0.25*PEAKI* + 0.75*SPKI*

if a QRS is detected in the searchback procedure [1], [3], [4] using *THRESHOLDI2*.

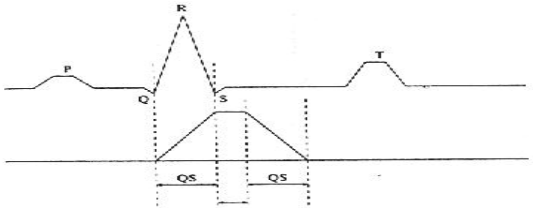

Fig.7.Upper plot-Schematic ECG signal;Lower plot Output of the moving-window integrator.

Fig.7 illustrates the effect of the window width on the output of the integrator and its relationship to the QRS width.

4. LabVIEW Pan-Tompkins algorithm implementation

After implementing the upper equations in LabVIEW we obtain following results Fig.8, Fig.9.

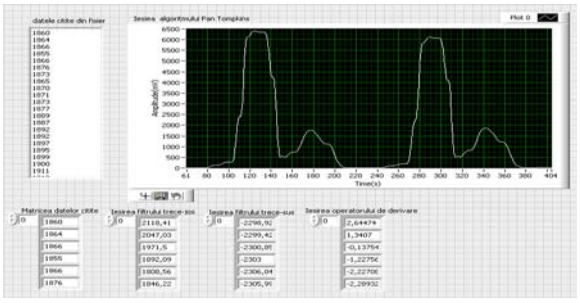

Fig.8. Pan-Tompkins algorithm front panel.

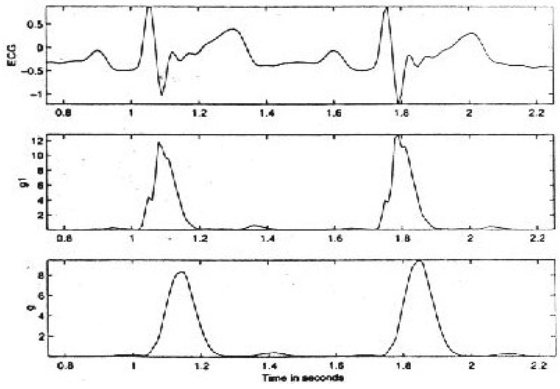

Fig.9. Results of the Pan-Tompkins algorithm.

a) two cycles of a filtered ECG;
b) output after ECG squaring;
c) the result of the final integrator.

4. Conclusion

The results obtained using LabVIEW for the implementation of the Pan-Tompkins algorithm is very fast and useful, because the ECG can be easily read and saved in a file and the filtering, squaring, integrating, applying the moving window can be accurately done. The peak detection is very important in diagnostic decision .

References:

[1]Rangayyan R.M., *Biomedical Signal Analysis*, Wiley-Intersciene, John Wiley & SONS, INC., 2002.

[2]Boashash B., *Time-Frequency Signal Analysis.*Wiley, New York, NY,1992.

[3]Pan J. and Tompkins WJ., A real-time QRS detection algorithm, *IEEE Transactions on Biomedical Engineering,* 32:230-236, 1985.

[4]Tompkins WJ., Biomedical Digital Signal Processing, *Prentice-Hall, Upper Saddle River,* NJ, 1995.